Available online at www.sciencedirect.com
SCIENCE DIRECT®
ELSEVIER
Journal of Chromatography A, 994 (2003) 1–12
JOURNAL OF CHROMATOGRAPHY A
www.elsevier.com/locate/chroma

Axial and radial diffusion coefficients in a liquid chromatography column and bed heterogeneity

R. Andrew Shalliker[a,b,c], B. Scott Broyles[a,1], Georges Guiochon[a,b,*]

[a]*Department of Chemistry, University of Tennessee, 552 Buehler Hall, Knoxville, TN 37996-1600, USA*
[b]*Chemical and Analytical Sciences Division, Oak Ridge National Laboratory, Oak Ridge, TN 37831-6120, USA*
[c]*Center for Biostructural and Biomolecular Research, University of Western Sydney, Richmond, NSW 1797 Australia*

Received 5 March 2001; received in revised form 19 December 2002; accepted 3 February 2003

Abstract

The axial and transverse diffusion coefficients of a band of iodine in a chromatographic column were measured optically as a function of time. It was found that the axial diffusion coefficient remains constant even when the edges of the sample band get close to the wall. By contrast, the radial diffusion coefficient decreases progressively with increasing time when the edges of the sample band leave the core region and begin to diffuse inside the wall region. The local axial and transverse diffusion coefficients of the band decrease from the column center toward the wall. Hence, the increase in local height equivalent to a theoretical plate observed in the region close to the wall must be explained by increasing mass transfer resistances and degree of heterogeneity of the bed.

Keywords: Diffusion coefficients; Stationary phases, LC; Packing density; Packed columns; Iodine

1. Introduction

Although they are the goal of the industry, highly efficient chromatographic columns, reproducibly packed with a highly uniform bed, have not yet been manufactured, let alone routinely so. Such columns should have a reduced height equivalent to a theoretical plate (HETP) of the order of unity. There are a few examples in the old literature of columns with such low reduced plate heights [1–4]. However, these were packed capillary columns for GC, manufactured and tested under highly unusual conditions. Actually, when chromatographic columns are evaluated, they prove to be heterogeneous, both axially and radially [5–7]. The better columns are the more homogeneous [7]. The top part of the bed is often less densely packed than its bottom part [5]. Variations of the packing density in the axial direction are slow and their extent small over the entire column length. Furthermore, in a radially homogeneous column, axial variations of the packing density would only cause a slight uniform increase of the band variance. However, a nonuniform radial distribution of the packing density has a more severe effect [7,8]. Such a distribution leads to a dramatic

*Corresponding author. Tel.: +1-865-974-0733; fax: +1-865-974-2667.
E-mail address: guiochon@novell.chem.utk.edu (G. Guiochon).
[1]Present address: Chemical and Analytical Sciences Division, Oak Ridge National Laboratory, Oak Ridge, TN 37831-6120, USA.

0021-9673/03/$ – see front matter
doi:10.1016/S0021-9673(03)00311-X

decrease in the column efficiency, because radial variations of the local bed density cause similar variations of the permeability, hence of the local mobile phase flow velocity. Instead of the zone remaining a uniform flat plug, these variations lead to a warping of the band [8]. Furthermore, the radial distribution of the local axial diffusion was observed to have a large amplitude [5–7,9], the local column efficiency being much lower in the region near the wall of the column than in that close to its axis. This contributes also to an increase in band broadening.

Radial variations of the local packing density may be attributed to two factors. First, the geometry of the packing in the wall region. The particles cannot penetrate the rigid wall surface, hence, the void fraction increases near the wall. Consequently, the solvent velocity in this region is much higher than the bulk flow velocity. This wall effect was documented recently [10] but its effect on the band profile is not yet substantiated, the amount of solute actually penetrating in this wall region being very low in most cases. The second factor that contributes to the radial variation of the packing density is related to the friction between the wall and the particles and between the particles themselves. Because this friction is strong, the stress distribution that is experienced during the packing process throughout the bed is most heterogeneous. This causes a radial heterogeneity of the column bed because, under friction-induced stress, the packing density increases as the distance to the wall decreases. This radial heterogeneity of the bed was observed in studies in which a dye marker was injected onto the column and the bed was extruded from the column container [11], or in which the mobile phase stream or the migrating bands were observed by nuclear magnetic resonance imaging [12] or optical means [13].

In this work we discuss the results of optical measurements of the radial and the axial diffusion coefficients and the relationships between their systematic variations and the heterogeneity of the distribution of the local packing density of the bed.

2. Theory

The simplest model of chromatography that is sufficiently realistic to account for the band profiles obtained in HPLC is the equilibrium–dispersive model [14]. This model was initially derived by Bohart and Adams [15]. Its solutions were studied first by Wicke [16,17] and later by Lapidus and Amundson [18], Van Deemter et al. [19], and Giddings [20] in the linear range, by Houghton [21], Haarhoff and van den Linde [22], and many others [14] under nonlinear conditions. This model accounts for the band broadening that takes place during their elution in liquid chromatography, by assuming that the combined effect of axial diffusion, eddy diffusion, and the mass transfer resistances is an axial dispersion [20]. Accordingly, the mass balance equation for one compound is written:

$$\frac{\partial C}{\partial t} + F \cdot \frac{\partial q}{\partial t} + u \cdot \frac{\partial C}{\partial x} = D_a \cdot \frac{\partial^2 C}{\partial x^2} \quad (1)$$

where C and q are the concentrations of the solute in the mobile and the stationary phases, respectively, t is the time, z the distance along the column of length L, u the mobile phase velocity, and F the phase ratio ($F = V_s/V_m = \varepsilon/(1-\varepsilon)$, where V_s is the volume of the stationary phase, V_m the volume of the mobile phase in the column and ε the total porosity of the column). In this model, mass transfer between phases in the column is assumed to be fast and the band migration along the column takes place practically under conditions of equilibrium. The coefficient of axial dispersion, D_a, is related to molecular and eddy diffusion and to the mass transfer kinetics [14].

Under static conditions ($u = 0$), the mobile and the stationary phases are in equilibrium at all times, hence are related by the isotherm equation, $q = f(C)$, and the mass balance equation reduces to a form of Fick's law:

$$\frac{\partial C}{\partial t} + F \cdot \frac{\partial q}{\partial t} = D_f \cdot \frac{\partial^2 C}{\partial x^2} \quad (2)$$

In the absence of flow, molecular diffusion is the only contribution to axial dispersion that remains. The coefficient D_f accounts for this diffusion. It differs from the molecular diffusivity D_m because of the tortuosity of a bed of particles and of the constriction of the flow channels that slow down molecular diffusion in a packed bed [20]. Even if the retention on the stationary phase is not negligible ($q \neq 0$), the axial dispersion term in Eq. (2) can be

replaced by the diffusion term, γD_m, with γ the bed tortuosity. Diffusion of compounds in a packed bed should be constant and independent of the location within the chromatographic column, at least provided that the bed of the chromatographic column be homogeneous, which it is not [5–13]. Because of the interactions between the column bed and the wall, the packing density has essentially a cylindrical symmetry [23], although this symmetry may be compromised in axial compression columns in the event that the head fitting is not perfectly parallel to the stationary phase bed upon initiation of bed compression [24].

In a homogeneous bed under static conditions, axial and radial molecular diffusion should take place at the same rate. In the absence of flow, the molecular diffusivity should be the same. If the apparent coefficients of axial and radial diffusion are different, this should be caused by different values of the tortuosity in the corresponding directions. We know that the packing density, hence F, increases from the core region of the bed to the wall [6,7], to drop suddenly to nearly 0 in the immediate vicinity of the wall [10,25]. Furthermore, because the bed is stressed more strongly at one end than at the other during the packing of the column [23], the bed is not axially homogeneous either. The heterogeneity of the bed causes diffusion to proceed at different rates in different parts of the column and also in different directions. A small sample injected into the bed may not grow into a sphere by molecular diffusion in the absence of flow. In the presence of flow at a finite velocity, dispersion proceeds at different rates in the direction of the flow and in the perpendicular directions. Mass transfer resistances and eddy diffusion combine with molecular diffusion to increase dispersion along the direction of the flow. Because of the stream splitting effect [26], eddy diffusion combines with molecular diffusion and enhances both axial and radial dispersion in the presence of flow [25,27]. Thus, a small sample injected in the bed may not grow into a symmetrical ellipsoid in the presence of flow because dispersion may proceed at different rates along different radial directions. The measurement of these deviations might provide estimates of the degree of heterogeneity of a column bed.

Variations of the packing density in the axial direction are relatively slow, except at the very ends of the column and when the stress applied during consolidation of the bed is high [23]. So, the axial variations of the bed density in a transparent column [13], which, being packed inside a glass tube, cannot stand a high mechanical stress, are negligible at the scale of the diameter of the droplets used in this study. Consequently, we may expect that the band variance in this column will increase at a nearly constant rate during its migration along the column. By contrast, the radial variations of the bed density are usually not negligible, even at the scale of the droplet. This is particularly true in the wall region, where the packing density and the tortuosity of the packed bed increase and, consequently, the rate of dispersion is expected to decrease significantly. Systematic investigations of the radial variation of the dispersion coefficient could give valuable information regarding the radial heterogeneity of the bed in the wall region. Note that accurate estimates of the average of the transverse dispersion coefficient were made by pulsed field gradient NMR [28]. Unfortunately, it was not possible to decrease sufficiently the volume within which the average is measured which prevented systematic investigations of the radial variation of the dispersion coefficient.

Let D_r and D_a be the apparent dispersion coefficients in the radial and the axial directions, respectively. Both coefficients can be measured experimentally through the determination of the evolution of the dimensions of a band in the radial and axial directions, respectively. The axial dispersion coefficient is simply related to the conventional column HETP, H, through the equation:

$$D_a = \frac{Hu}{2} = \frac{Lu}{2N} \tag{3}$$

where L is the column length and N its efficiency. Under linear chromatographic conditions [29], the variance of a Gaussian band, σ^2, follows the classical relationship:

$$\sigma^2 = HL = 2Dt_0 \tag{4}$$

where t_0 is the retention time of an unretained solute. Under static flow conditions, t_0, is the period of time during which the measurements of the band variance are carried out and D_a would be replaced by D_f. Because the injected band has a finite width and

series of measurements are made on this band while it is inside the column [13], by taking actual photographs of the band, the two dispersion coefficients are determined according to the following two equations derived from Eq. (4):

$$D_a = \frac{(\sigma_2^2 - \sigma_1^2)_a}{2(t_2 - t_1)} \quad \text{(a)}$$
$$D_r = \frac{(\sigma_2^2 - \sigma_1^2)_r}{2(t_2 - t_1)} \quad \text{(b)} \qquad (5)$$

where σ_2^2 and σ_1^2 are the variances of the sample band at times t_2 and t_1, respectively. This procedure accounts for the influence of the initial band width (see below).

2.1. Experimental determination of the diffusion coefficients

In chromatography, we must make a clear distinction between dispersion and diffusion coefficients. Both terms are related to and derived from evaluations of band broadening. In this work, however, measurements are made under static conditions, with no flow. Band broadening occurs solely as a result of molecular diffusion in the bed because there is no flow of the mobile phase ($u = 0$).

It is difficult to measure dispersion, let alone diffusion, in chromatographic columns. The corresponding contribution arises solely from factors characterizing the bed packing. However, other contributions arise during migration of the solute from the injector, the connecting tubings, the head fitting, the inlet and outlet frits, the end frit, more tubings, and the detector. The total band variance is the sum of the contributions of all these effects. Assuming that the solute is injected as a droplet into the bed center, the contributions to band broadening of the inlet head and frit are removed, that of the tubings reduced. As long as the solute elutes under ''infinite diameter column'' conditions, the wall effect contribution is also eliminated. Further reductions of the band variance may be made if detection is carried out on-column, thereby avoiding the contributions of all post-column tubings, of the outlet head and frit, and of the detector flow cell. Consequently the total band variance may be found according to:

$$\sigma_{total}^2 = \sigma_{inj}^2 + \sigma_{col}^2 \qquad (6)$$

In order to determine the dispersion or diffusion coefficients from the progressive broadening of a band, we need to measure on-column the true band variance of a sample injected directly into the bed and to do so at successive time intervals. This process will allow the elimination of the variance contributions associated with the instrument, leaving only the change in variance associated with the packed bed.

Obviously, in the opaque environment of a stainless steel tube, it is difficult to observe an actual solute band. This explains why the actual observation of bands during their migration is unusual and why studies involving on-column dispersion measurements are few. Some examples may be found in the literature [10,13,30,31]. Because bands cannot be conveniently observed directly, accurate on-column evaluations of axial dispersion are difficult. Such measurements are typically made by monitoring the composition of the outlet stream of mobile phase exiting the column with an on-line detector. This detector can monitor the bulk effluent as in conventional applications, or it can monitor the local concentration of the outflowing stream if it is small and placed directly at the column outlet or just before it [6,7]. Even in this last case, it is not possible to derive the bed variance contribution since the injection contribution cannot be derived simply from a single, post-column determination, Actually, the contributions to band broadening of the injection process and of the inlet tubing, head, and frit may be more important than usually realized [32–34]. Finally, to measure the coefficient of radial dispersion, it is necessary to perform local injections of the sample, so that there is a radial concentration gradient. The initial or injection variance contribution must also be measured and subtracted from the total band variance. Otherwise, derivation of the radial dispersion from the signals detected would overestimate the contribution of the column packing to both radial and axial dispersion. Accordingly, if the bands are eluted to be detected, radial or axial dispersion are difficult to measure accurately.

NMR measurements of bands migrating along packed beds have yielded useful information allowing direct determination of on-column axial and

radial dispersion and diffusion [28,35,36]. It proved to be more convenient and more accurate to carry out the measurements of axial and radial dispersion coefficients by pulsed field gradient NMR than by direct imaging [12,26,37,38]. Diffusion effects could be separated from flow effects as a result of a phase shift within the signal. Using this method, Tallarek et al. [39] were able to calculate the coefficient of self-diffusion for acetone ($4.08 \cdot 10^{-5}$ cm^2 s^{-1}), acetonitrile ($2.75 \cdot 10^{-5}$ cm^2 s^{-1}), methanol ($1.98 \cdot 10^{-5}$ cm^2 s^{-1}) and water ($1.98 \cdot 10^{-5}$ cm^2 s^{-1}).

An alternative method of evaluating the axial and radial dispersion coefficients in the presence or absence of flow is to look inside a chromatographic column made of a transparent (glass) tube and containing a transparent bed. This is possible if mobile and stationary phases have the same refraction index. This technique was previously described in the literature [31–34]. Injection of a colored solute onto the column allows easy evaluation of the band width at different times, with or without flow [10,13,32–34]. This is the method used in the present work.

3. Experimental

Transparent chromatographic beds are obtained by packing a borosilicate tube of proper dimensions with a C_{18} bonded porous silica and operating it with a mobile phase of same refractive index. We found carbon tetrachloride to be most practical for this application in spite of its toxicity [13]. The whole equipment was kept under a hood which is kept closed most of time. Other combinations of stationary phase and solvent are possible but were not investigated. Minimizing the difference between the temperature coefficients of the refractive indices of the solid and the liquid phases seem to be the most critical issue in this choice.

3.1. Chemicals

Reagent-grade carbon tetrachloride was obtained from Sigma (St. Louis, MO, USA); reagent grade methanol and HPLC-grade dichloromethane from Mallinckrodt (Paris, KY, USA). Iodine (99.9%) was from General Chemical Division (New York, NY, USA). All the mobile phases were sparged with helium during the experiments.

3.2. Columns and packing material

All chromatographic experiments were performed on a 100×17 mm (I.D.) borosilicate (Pyrex) glass column supplied by Omni (Cambridge, UK). The column end fittings were machined from Delrin plastic at the University of Tennessee workshop. These fittings included a fixed length outlet fitting and an adjustable inlet fitting that allowed axial compression of the column. Stainless steel frits having a diameter of 15.9 mm and a thickness of 1.57 mm were obtained from Bodman (Aston, PA, USA).

The stationary phase used was YMC C_{18} silica (Kyoto-Fu 613 Japan). The particles of this packing material are spherical, with a particle size distribution given as 15–30 μm and an average particle size of 21 μm. The column was slurry packed in a downward configuration with methanol as both the slurry and the packing solvent. Dichloromethane was used as the displacement solvent. The slurry was pushed into the column and consolidated by a steady stream of methanol at a flow-rate of 9 ml min^{-1}. The inlet pressure did not exceed ca. 18 atm (250 p.s.i.) to avoid breaking the glass column. The head fittings were assembled and inserted into the head of the column. The head fitting was then tightened to a torque of 0.2 m kg^{-1} and allowed to set overnight before use. To improve visualization and minimize the cylindrical lens effect, the entire column assembly was placed into a viewing cell having a square cross-section and closed with four vertical silica plates. This cell assembly was described in a previous communication [13].

3.3. Sample injection

Solutions of iodine in carbon tetrachloride (12 g l^{-1}) were used as the sample. At this concentration, the solute zones are sufficiently colored. A detailed observation of the zones obtained upon the injection of small volumes (less than the 20 μl used in this work) is possible during their entire elution. Central point injections were achieved by inserting a needle

through the inlet frit at a distance of approximately 0.5 cm below the head fitting. The head fitting was then inserted into the bed, with minimal disturbance to the column inlet. A sample of the iodine solution was injected onto the column inlet. This zone was eluted into the central region of the bed. At this point the flow was stopped and the sample band was photographed at regular intervals over the next 50-min period. To prevent fluid flow, the outlet of the column was capped during this period.

3.4. Equipment

The chromatographic system consisted of two high-performance liquid chromatographic (HPLC) pumps (model 510, Waters Associates, Milford, MA, USA) controlled by a Waters automated gradient controller. The mobile phase was pure carbon tetrachloride. Sample visualization of the band profiles was achieved using two Pentax ZX-M SLR 35-mm cameras fitted, one with a Promaster 100-mm macro lens, the other with a Makinon 80–200-mm macro zoom lens. The two cameras were located at right angle. The opposite two windows of the viewing cell were illuminated by fluorescent tubes placed behind sheets of translucent glass.

Kodak Ektachrome 200 ASA Professional slide film was used throughout. The photographic images were digitized using a Nikon CoolScan II (Nikon, Melville, New York, NY, USA) film scanner. All images were acquired at the maximum resolution of the scanner (2700 dots $in.^{-1}$; 1 in. = 2.54 cm). Adobe Photoshop 5.0 (Adobe Systems, San Jose, CA, USA) was used to perform image manipulation. Further analysis (e.g. the determination of the optical density profiles along selected axial and radial directions of the band photographs) was done using SigmaScan Pro 4.01 (Jandel Scientific, San Rafael, CA, USA) image analysis software.

4. Results and discussion

4.1. Image collection and analysis

Previous studies reported all the relevant details of the processes of image collection, of the subsequent analysis of the photographic images obtained, and of their conversion into digital format [13]. In this study, the protocols previously discussed were strictly adhered to, except for one modification which had to be made to allow the precise determination of the solute concentrations. Some further discussion of this change is warranted.

The iodine sample was injected into the upper part of the bed of the chromatographic column, using the central point source injection described earlier. This resulted in a nearly perfectly spherical band, as illustrated in the series of photographs shown in Fig. 1. These photographs depict the diffusion of the sample in the central region of the column over a time period of 45 min. Fig. 1a confirms the symmetry of the zone of the injected sample. The axial and radial concentration profiles of these bands were directly derived from the photographs. These two profiles are shown in Fig. 2a and b, respectively. In previous studies, the process of deriving the concentration profiles from the optical density profiles of the bands involved calibration against a series of known standard concentration solutions that were equilibrated within the packed bed until elution of the breakthrough front. Since the column is cylindrical, corrections for the variable path length were necessary. This calibration process resulted in the non-linear calibration curve described in the following equation:

$$C = e^{a+b\sqrt{I}} \tag{9}$$

This calibration curve has two coefficients, a and b, that both depend on the radial location. In previous experiments [13], these two coefficients were determined at a few predefined radial locations. However, these experiments used broad injections, covering the whole radial cross-section of the column, and only the axial concentration profiles along a few parallel to the column axis were needed. In the present work, measurements of the radial and axial concentration profiles of the zone were needed. In order to evaluate the extent of radial diffusion, these measurements were made as a function of time rather than of the migration distance of the band center along the bed. So, it was insufficient to use the calibration coefficients determined as before but it became necessary to measure them with a better radial definition. To obtain the values of a and b as a

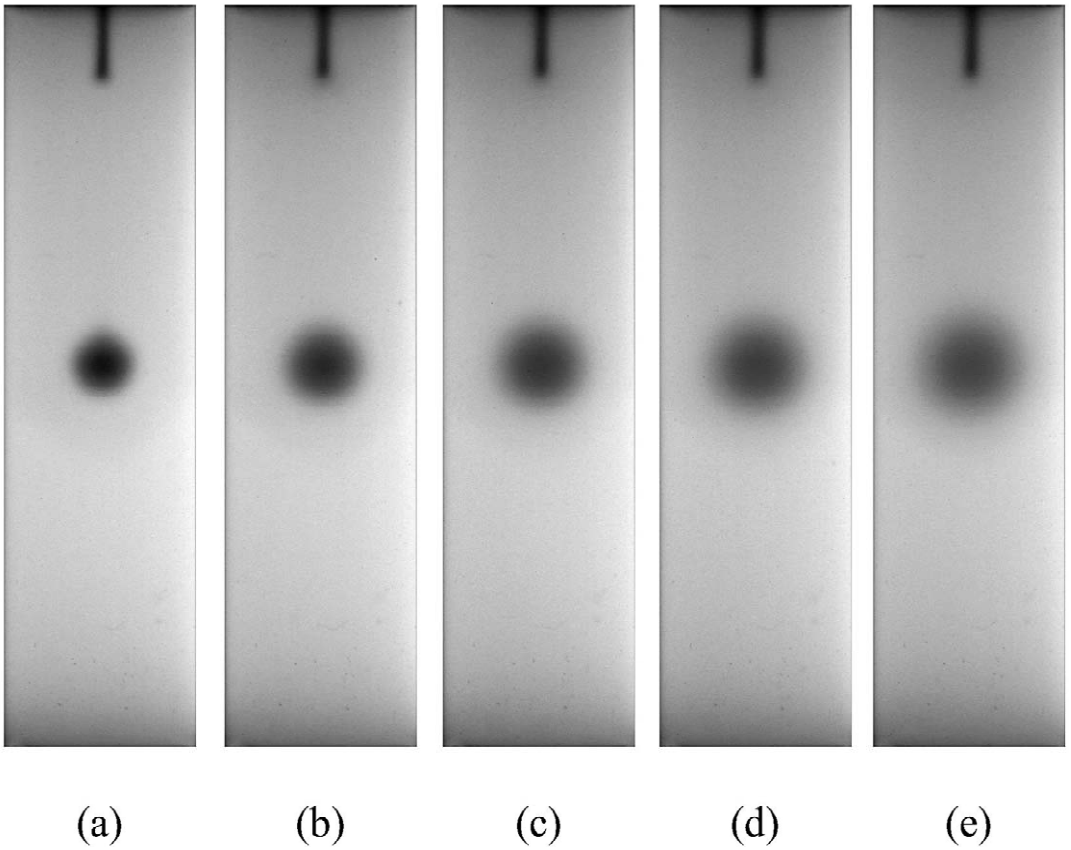

Fig. 1. Photographs of a standing iodine sample. (a–d) Camera A; (e) camera B. Time after the end of the injection: (a) 30 s; (b) 10 min 30 s; (c) 20 min 30 s; (d) 30 min 30 s; (e) 40 min 30 s.

function of the radial position, the experimental data were obtained as before, then they were plotted versus the radial distance in the column (Fig. 3a and b). The calibration coefficients at any radial location across the column were derived from these curves. Note that these curves are not perfectly symmetrical about the column axis. This more than likely is a reflection upon our inability to perfectly align the head fitting on top of the chromatographic column parallel to the bed head prior to bed compression. Subsequently, the bed undergoes compression in a non-symmetrical manner [24]. Following the determination of the coefficients and the subsequent radial concentration distribution, the concentration profile of the sample band in the radial direction required the normalization of the chromatographic profile with respect to the column cylinder diameter at each of the respective radial locations for which the coefficients a and b were determined. This allowed the determination of all the concentration profiles.

4.2. Determination of the diffusion coefficients

The band variance of each of the concentration profiles displayed in Fig. 2 were calculated. Note than the range of the band widths in Fig. 2b extends from approximately 0.3 to 0.8 column diameter. In this range, the radial diffusion coefficient is expected significantly to depend on the radial distance [5]. Fig. 4 illustrates the variation of the band variance as a function of the time elapsed, in both directions. In the axial direction, a linear relationship ($R^2 = 0.999$) is observed between band variance and time. By

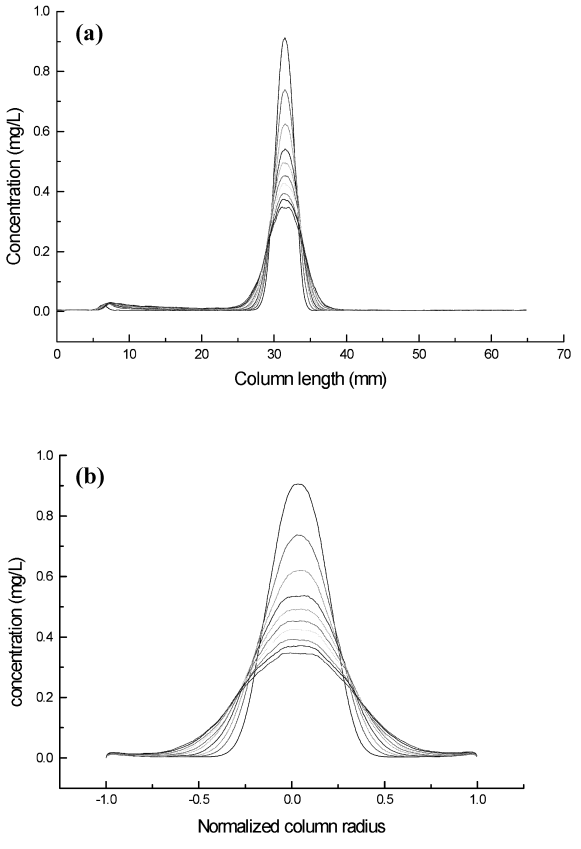

Fig. 2. Concentration profiles across a droplet of iodine solution standing in the chromatographic column (no flow-rate). (a) Profiles in the axial direction (b). Profiles in the radial direction.

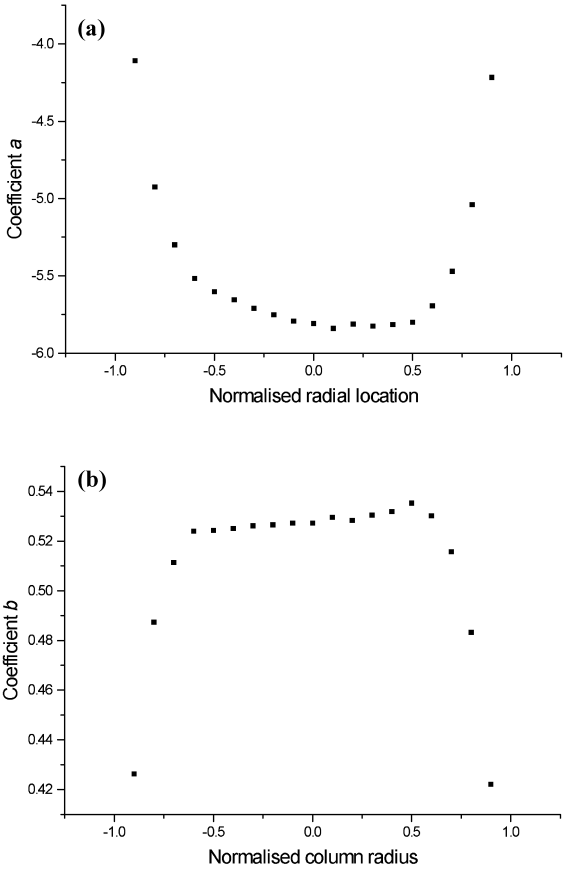

Fig. 3. Plots of the coefficients of the calibration equation (Eq. (9)) as functions of the radial position. (a) Coefficient *a*. (b) Coefficient *b*.

contrast, in the radial direction, this relationship is not linear. Using Eqs. (5a) and (5b), the diffusion coefficients in both directions were calculated from the graphs in Fig. 4. The results are plotted in Fig. 5. The axial diffusion coefficient is nearly constant, except for an initial decrease, which we expect may be due to relaxation within the column after the flow of mobile phase was stopped. The essentially constant diffusion coefficient was in agreement with the linear relationship observed between time and the variance of the band profile (Fig. 4). This confirms other experimental results indicating that the packing density is nearly constant along the column axis [23,40] and that the axial diffusion coefficient is also constant [5,32–34,39].

Using Eq. (5b), an empirical diffusion coefficient in the radial direction was calculated from the data in

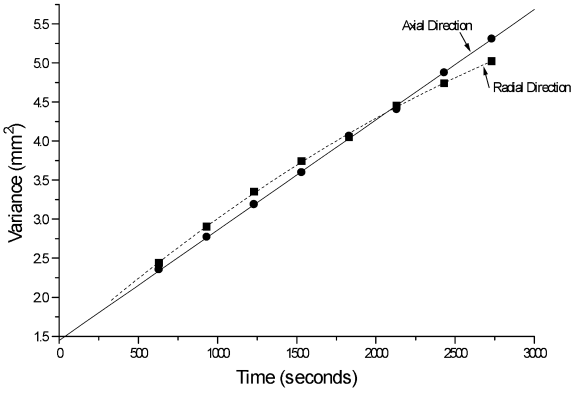

Fig. 4. Plots of the axial and radial variances of the band versus time.

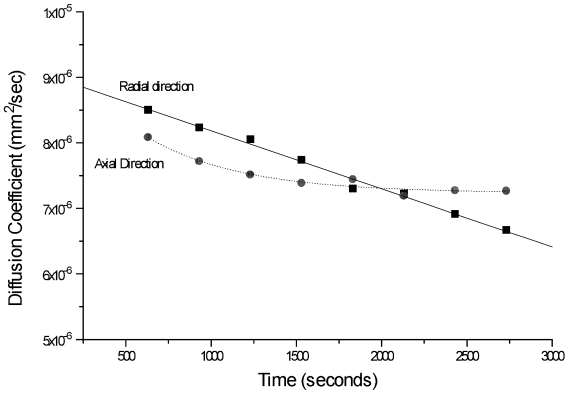

Fig. 5. Plots of the axial and radial diffusion coefficients versus time.

Fig. 4. The values obtained are plotted with respect to time and are shown in Fig. 5. This coefficient exhibits a continuous and almost linear decrease as the solute diffuses closer to the column wall. This result is consistent with the radial distribution of the packing density of the bed previously reported and its consequences on the radial distribution of the local HETP [6,7]. As the solute nears the wall, the packing density increases and, consequently, the bed tortuosity increases, hence, the radial diffusion coefficient measured in the bed decreases. The consequences of bed heterogeneity in the radial direction are catastrophic with regards to solute band broadening. Photographic images of solute zones migrating along a chromatography column at various radial locations illustrate this result and are shown in Fig. 6. In Fig. 6, at the point of initial solute injection into the bed of the column, all solute zones were uniform and spherical (not shown). However, by the time the solute had migrated to near the column outlet the solute zones in the regions nearing the wall were distorted. In contrast the solute zone migrating along

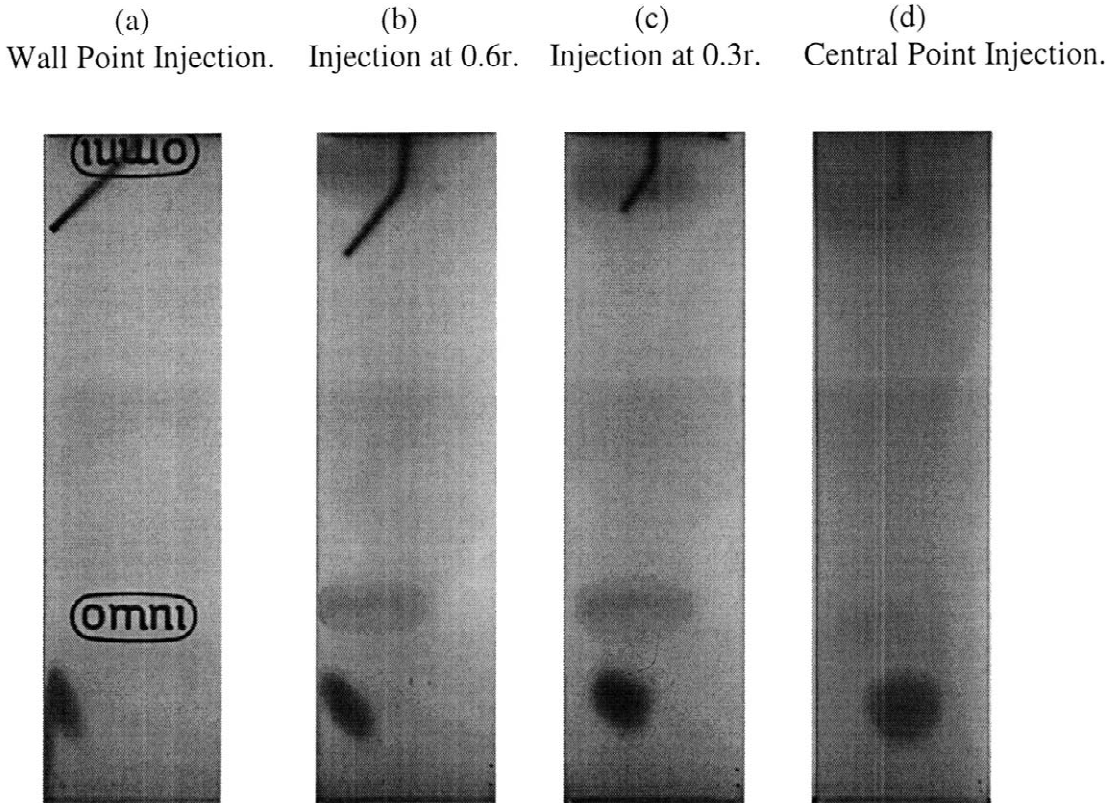

Fig. 6. Photographic images of solute bands migrating along various radial sections of the chromatography column. (a) Wall point injection, (b) injection at 0.6r, (c) injection at 0.3r, and (d) a central point injection.

the central section of the column remained spherical. Furthermore, this distortion became more significant for solute nearest the wall.

Before interpreting these results, we need to discuss their accuracy. First, regarding the radial coefficient, we note that it is an average and that the calculation procedure biased the estimate obtained toward markedly too large values. Even when the band reaches relatively close to the column wall, the bulk of the solute amount is in the core region. The coefficient D_r is nearly constant in this core region but depends on the radial distance for $r > 0.50$. In order for the average of D_r to decrease with increasing radial distance as it does (Table 1 and Fig. 5), the local value of D_r can only decrease markedly faster. By definition of the local HETP, it is the proportionality coefficient between the differential increase of the band variance and the differential element of migration [20]:

$$d\sigma^2 = H\,dx = Hu\,dt = 2D(r)\,dt \quad (10)$$

However, the band variance corresponding to a diffusion coefficient that is a function of the radial distance can be obtained only as a volume integral, with the axial and radial positions as the integral variables. This leaves little hope of deriving a reasonable estimate of $D(r)$, because such integral problems are usually ill-posed and always difficult to solve. Because the upper and lower parts of the band are well in the core region and where $D(r)$ is nearly constant, the estimate of the axial diffusion coefficient of the band is less biased. The average value (Table 1) is $7.53 \cdot 10^{-6}$ cm^2 s^{-1}. This estimate is obviously lower than the molecular diffusivity.

Table 1
Apparent diffusion coefficients of iodine

Time (s)	D_r ($\times 10^{-6}$, cm^2 s^{-1})	D_a ($\times 10^{-6}$, cm^2 s^{-1})
630	8.50	8.09
930	8.24	7.72
1230	8.05	7.51
1530	7.74	7.39
1830	7.30	7.45
2130	7.23	7.19
2430	6.91	7.28
2730	6.67	7.27

Calculations from the correlation of Wilke and Chang [41] gave for iodine in pure carbon tetrachloride a value of $2.30 \cdot 10^{-5}$ cm^2 s^{-1} which is too large. The average experimental values of the axial diffusion coefficient of iodine in carbon tetrachloride obtained by Stokes et al. [42] and used by Wilke and Chang in their correlation [41] is only $1.50 \cdot 10^{-5}$ cm^2 s^{-1} (both values at 25 °C; our experiments were run at ca. 22 °C; a 3 °C difference in temperature may correspond to a negligible 1% change in diffusion coefficients) [41]. This difference between experimental and calculated values is well in excess of the average deviation of 12% reported but it was not discussed [42]. Because the value reported by Stokes et al. [42] is of experimental origin, we will retain it. Its ratio with the axial diffusion coefficient in our column is 1.99 ($\gamma = 0.50$), a value that is somewhat larger than usual estimates of the bed tortuosity, generally assumed to be closer to 1.5 [20,43]. In a recent investigation of the mass transfer of the solvent in an HPLC column, using an NMR method, Tallarek et al. [44] estimated the value of (for a packed bed at 0.65 (and that of the particles themselves at approximately 0.40). Our value of γ, although smaller than usual, is not exceptional. In their classical paper on obstructive factors, Knox and McLaren [43] reported values of (between 0.45 and 0.76 for columns packed with irregular particles and between 0.48 and 0.82 for columns packed with spherical particles. Later, Hawkes and Steed [45] summarized data from ten different publications and found values between 0.49 and 0.80 for glass bead columns. Although we have striven to control the measurements errors [13], our ignorance of the factors affecting γ prevents us from offering an explanation for this result.

Previous studies by Mills et al. [46] and Baumeister et al. [28] also reported differences between the radial and axial diffusion coefficients derived from NMR imaging measurements. In their studies, diffusion was 2–7% higher in the axial than in the radial direction. As explained earlier, it is difficult to interpret correctly the results and a quantitative comparison between values obtained with different methods would not be meaningful. However, the results obtained support our argument that such differences may be attributed to the differences in the radial packing density.

5. Conclusion

In conclusion, radial and axial diffusion coefficients of iodine in a chromatographic column eluted with carbon tetrachloride were measured and found to exhibit markedly different behaviors. There was an almost constant value for the diffusion constant in the axial direction as opposed to a linear decrease in the diffusion coefficient in the radial direction. This can be explained only by a bed tortuosity increasing from the column center toward the wall, in the wall region.

Although we must caution regarding the interpretation of results based on the behavior of a single column, results that have a limited accuracy, our results are important because they are just the opposite of what one might have expected. The diffusion coefficient is markedly lower in the wall region than in the core region. On the other hand, we know that the axial diffusion coefficient and the local HETP are much higher near the column wall than in the column core. This may be explained only by a much higher mass transfer resistance in the wall region, particularly for transfers in the mobile phase. The increased HETP in the wall region may be explained also by a higher degree of heterogeneity of the flow velocity. This is further supported by bed compression studies which have shown that the bed undergoes a greater degree of consolidation near the wall region [47].

Acknowledgements

This work was supported in part by grant DE-FG05-88-ER13869 of the US Department of Energy and by the cooperative agreement between the University of Tennessee and the Oak Ridge National Laboratory.

References

[1] J.C. Giddings, R.A. Robison, Anal. Chem. 34 (1962) 885.
[2] J.C. Giddings, Anal. Chem. 35 (1963) 1338.
[3] I. Halasz, E. Heine, Nature 194 (1962) 971.
[4] J.C. Sternberg, R.E. Poulson, Anal. Chem. 36 (1964) 1492.
[5] G. Guiochon, T. Farkas, H. Guan-Sajonz, J.-H. Koh, M. Sarker, B.J. Stanley, T. Yun, J. Chromatogr. A 762 (1997) 83.
[6] T. Farkas, M.J. Sepaniak, G. Guiochon, AIChE J. 43 (1997) 1964.
[7] T. Farkas, G. Guiochon, Anal. Chem. 69 (1997) 4592.
[8] M.S. Smith, G. Guiochon, J. Chromatogr. A 827 (1998) 241.
[9] C.H. Eon, J. Chromatogr. 149 (1978) 29.
[10] R.A. Shalliker, B.S. Broyles, G. Guiochon, J. Chromatogr. A 888 (2000) 1.
[11] T. Yun, G. Guiochon, J. Chromatogr. A 760 (1997) 17.
[12] U. Tallarek, K. Albert, E. Bayer, G. Guiochon, AIChE J. 42 (1996) 3041.
[13] R.A. Shalliker, B.S. Broyles, G. Guiochon, Anal. Chem. 72 (2000) 323.
[14] G. Guiochon, S.G. Shirazi, A.M. Katti, Fundamentals of Preparative and Nonlinear Chromatography, Academic Press, Boston, MA, 1994.
[15] G.S. Bohart, E.Q. Adams, J. Am. Chem. Soc. 42 (1920) 523.
[16] E. Wicke, Kolloid Z. 86 (1939) 295.
[17] E. Wicke, Kolloid Z. 90 (1940) 156.
[18] L. Lapidus, N.R. Amundson, J. Phys. Chem. 56 (1952) 984.
[19] J.J. van Deemter, F.J. Zuiderweg, A. Klinkenberg, Chem. Eng. Sci. 5 (1956) 271.
[20] J.C. Giddings, The Dynamics of Chromatography, Marcel Dekker, New York, 1960.
[21] G.J. Houghton, J. Phys. Chem. 67 (1963) 84.
[22] P.C. Haarhoff, H.J. van der Linde, Anal. Chem. 38 (1966) 573.
[23] G. Guiochon, E. Drumm, D. Cherrak, J. Chromatogr. A 835 (1999) 41.
[24] R.A. Shalliker, V. Wong, B.S. Broyles, G. Guiochon, J. Chromatogr. A 977 (2002) 213.
[25] G.E. Mueller, Chem. Eng. Sci. 46 (1990) 706.
[26] U. Tallarek, E. Bayer, G. Guiochon, J. Am. Chem. Soc. 120 (1998) 1494.
[27] P.G. Saffman, J. Fluid Mech. 7 (1960) 194.
[28] E. Baumeister, U. Klose, K. Albert, E. Bayer, G. Guiochon, J. Chromatogr. A 694 (1995) 321.
[29] E.V. Dose, G. Guiochon, Anal. Chem. 61 (1990) 1723.
[30] M.S. Tswett, Tr. Protok. Varshav. Obshch. Estestvoistpyt., Otd. Biol., 14 (1903, publ. 1905) 20. On the new Category of Adsorption Phenomena and their Applications in Biochemical Analysi, Reprinted and Translated in G. Hesse and H. Weil, ''Michael Tswett's erste chromatographische Schrift,'' Woelm, Eschwegen, 1954.
[31] J.J. Kirkland, in: N.J. Fina (Ed.), Proceedings of the First Philip Morris Scientific Symposium, Philip Morris, New York, 1973.
[32] B.S. Broyles, R.A. Shalliker, G. Guiochon, J. Chromatogr. A 855 (1999) 367.
[33] B.S. Broyles, R.A. Shalliker, G. Guiochon, J. Chromatogr. A 865 (1999) 83.
[34] R.A. Shalliker, B.S. Broyles, G. Guiochon, J. Chromatogr. A 865 (1999) 73.
[35] M. Ilg, J. Maier-Rosenkranz, W. Müller, E. Bayer, J. Chromatogr. 517 (1990) 263.

[36] U. Tallarek, E. Baumeister, K. Albert, E. Bayer, G. Guiochon, J. Chromatogr. A 696 (1995) 1.
[37] E. Fernandez, C. Grotegut, G. Braun, J. Phys. Fluids 7 (1995) 468.
[38] E. Fernandez, T. Norton, W. Jung, J. Tsavalas, Biotechnol. Prog. 12 (1996) 480.
[39] U. Tallarek, D. van Dusschoten, T. Scheenen, H. Van As, E. Bayer, G. Guiochon, U.D. Neue, AIChE J. 44 (1998) 1962.
[40] B.G. Yew, E.C. Drum, G. Guiochon, in: Proceedings of the Fourth International Conference on Constitutive Laws for Engineering Materials: Experiment, Theory, Computation and Applications, Troy, NY, 1999, p. 513.
[41] C.R. Wilke, P. Chang, AIChE J. 1 (1955) 264.
[42] R.H. Stokes, P.J. Dunlop, J.R. Hall, Trans. Faraday Soc. 49 (1952) 886.
[43] J.H. Knox, L. McLaren, Anal. Chem. 36 (1964) 1477.
[44] U. Tallarek, D. van Dusschoten, H. Van As, E. Bayer, G. Guiochon, J. Phys. Chem. B 102 (1998) 3486.
[45] S.J. Hawkes, S.P. Steed, J. Chromatogr. Sci. 8 (1970) 256.
[46] R. Mills, J. Phys. Chem. 77 (1973) 1.
[47] B.G. Yew, J. Ureta, E.C. Drumm, G. Guiochon, AIChE J. (2003) in press.